

Analysis of Dipole Matrix Element in Quantum Well and Quantum Cascade Laser under the Influence of External Magnetic Field

Aleksandar Demić¹, Jelena Radovanović¹, Vitomir Milanović¹

Abstract: We present a method for modeling nonparabolicity effects (NPE) in quantum nanostructures by using second order perturbation theory. We will analyze application of this model on a quantum well without external electric field and a quantum cascade laser (QCL). This model will allow us to examine the influence of magnetic field on dipole matrix element in QCL structures which will give better insight how NPE can disrupt gain of QCL structures.

Keywords: Quantum cascade lasers, Nonparabolicity effects.

1 Introduction

Nonparabolicity effects (NPE) in the conduction band (CB) of a semiconductor quantum well (QW) material have an essential role in modeling of electronic structure of multiple QW such as quantum cascade laser (QCL). Several approaches exist in literature, e.g., the inclusion of energy-dependent electron effective mass. Ekenberg in [2] determined the coefficients in the expansion of the dispersion relation up to the fourth order in wavevector, by using 14-band $\mathbf{k} \cdot \mathbf{p}$ calculation presented in [1]. This results in a fourth-order differential equation with boundary conditions obtained by double integration, which fulfill the requirement for probability current conservation [3]. In [4] the authors presented the model from [2, 3] and its application to QCL structures by using the transfer matrix method (TMM). Modeling of NPE represents a nonlinear eigenvalue problem, thus it is preferable to develop an approximate solution.

QCL structures are powerful light sources emitting from mid-infrared (MIR) to THz frequencies that have turned out to be efficient and reliable in free-space communications, medical diagnostics, and chemical sensing [5 – 9]. By engineering of the active region, it is possible to obtain a wide range of operating wavelengths from $3\mu\text{m}$ up to $250\mu\text{m}$. The lasing wavelength is defined by separation of laser energy states, and for THz frequencies it is clear

¹School of Electrical Engineering, University of Belgrade, 73 Bulevar kralja Aleksandra, 11020 Belgrade, Serbia; E-mails: alexandardemic@yahoo.com; radovanovic@etf.bg.ac.rs; milanovic@etf.bg.ac.rs

that the energy difference is very small (around 10meV) and thus any shift in energy can make modeling of these structures more demanding.

In this paper we use the model from [2 – 4] and apply the second order perturbation theory in order to model energy corrections more accurately. In [2], Ekenberg applied first order perturbation theory for energies, and the authors in [4] only used the unperturbed Hamiltonian from [2], while in this paper we will present a more precise treatment through the second order perturbation theory. We will apply this model to QW structure which yields analytic solution, then consider the QCL structure for which this model can have a great importance, especially for higher frequencies.

The second order perturbation theory generally takes into account overlapping between any two states in the energy spectrum. We are interested only in corrections of bound states energies and it is customary to consider just the overlap integrals between the bound states, since higher states have smaller effect. In the example of QW (without the presence of electric field) we will consider the entire spectrum, by modeling the bound states with NPE, and the continuum states from Schrödinger equation. We will also consider the first order correction for the wavefunctions and this will allow us to study the effect of magnetic field on dipole matrix element, or in another sense, on the gain of QCL.

It is also important to note that the model from [2 – 4] cannot be used for all bound states, as explained in [4]. For GaAs structures with parameters from [2] the model is applicable for energies less than 213meV, and the limiting energy varies on parameters of the structure. This energy represents the turning point of the dispersion relation. We claim the applicability of the model up to max energy of the dispersion relation presented in [4] which is 384meV.

2 Theoretical Consideration

We will focus on Hamiltonian presented in [2] in presence of magnetic field which can be written as:

$$\begin{aligned} \hat{H} &= \hat{H}_P + \hat{H}_{NP}, \quad \hat{H}_P = \hat{H}_0 + \hat{H}' \\ \hat{H}_{NP} &= (2\alpha_0(z) + \beta_0(z)) \frac{1}{2} \left\{ \hat{k}_x, \hat{k}_y \right\}^2 + \alpha_0(z) (\hat{k}_x^4 + \hat{k}_y^4), \\ \hat{H}_0 &= \hat{k}_z^2 \alpha_0(z) \hat{k}_z^2 + \frac{\hbar^2}{2} \hat{k}_z - \frac{1}{m^*(z)} \hat{k}_z + V(z), \quad \hat{H}' = \left(j_n + \frac{1}{2} \right) \frac{eB\hbar}{\hat{M}(z)}, \\ \frac{1}{\hat{M}(z)} &= \frac{1}{m^*(z)} + \frac{2}{\hbar^2} \hat{k}_z (2\alpha_0(z) + \beta_0(z)) \hat{k}_z. \end{aligned} \quad (1)$$

Here, \hat{H}_P represents the parabolic part of the Hamiltonian and \hat{H}_{NP} the non-parabolic part can be treated with the second order perturbation theory (first correction vanishes) and this was done in [2]. In this paper we focus on \hat{H}_P , and apply the second order perturbation theory. Hence \hat{H}_P can be represented as a sum of the unperturbed Hamiltonian \hat{H}_0 and the perturbed one \hat{H}' . The coefficients α_0 and β_0 are nonparabolicity parameters given in [2], B is the magnetic induction of external magnetic field, $V(z)$ is the potential of the structure, $\hat{k}_x, \hat{k}_y, \hat{k}_z$ are the wavevector components operators, $m^*(z)$ is the effective mass and j_n is the Landau level index.

The Hamiltonian in (1) operates on the envelope wavefunction $\eta_n(z)$ and we treat \hat{H}_P and \hat{H}_{NP} separately. For \hat{H}_P we first we solve the eigenvalue problem with the unperturbed Hamiltonian $\hat{H}_0\eta_{n0}(z)=E_n^{(0)}\eta_{n0}(z)$ (index 0 denotes zeroth order correction, while $n=1, 2, \dots$ represent the bound state energy indices) and use the wavefunctions $\eta_{n0}(z)$ as a basis for perturbation theory. The first order correction for energy is given in [2] as

$$\Delta E_n^{(1)} = \left(j_n + \frac{1}{2} \right) \frac{eB\hbar}{m_{||}}, \quad (2)$$

where j_n is Landau level index and

$$\frac{1}{m_{||}} = \int_{-\infty}^{\infty} \eta_{n0}^* \frac{1}{\hat{M}(z)} \eta_{n0} dz.$$

The second order correction for energy can be determined as

$$\Delta E_n^{(2)} = \left[\left(j_n + \frac{1}{2} \right) eB\hbar \right]^2 \sum_{k \neq n} \frac{|M_{nk}|^2}{E_n^{(0)} - E_k^{(0)}}, \quad n \neq k,$$

where

$$M_{nk} = \int_{-\infty}^{\infty} \eta_{n0}^* \frac{1}{\hat{M}(z)} \eta_{k0} dz, \quad n \neq k. \quad (3)$$

It is clear that (3) should be calculated using all the states in the spectrum, both bound and continuum. We are mainly interested in corrections of the bound states energies, hence higher energies should have much less effect, on the other hand it is obvious that the correction in (3) depends on the squared value of magnetic induction, hence higher energies may enhance this model. For that reason we will consider equation (3) for bound states only, and add

separately the correction for continuum states. The equation for continuum correction is the same as (3) but we just add index *cont* in it ($M_{nkcont}, \eta_{k0cont}$). Since M_{nkcont} consists of continual values, the sum in (3) becomes an integral and the correction for continuum states reads

$$\Delta E_{ncont}^{(2)} = \left[\left(j_n + \frac{1}{2} \right) eB\hbar \right]^2 \frac{L}{\pi} \int_0^\infty \frac{|M_{nkcont}|^2}{E_n^{(0)} - E_k^{(0)}} dk_z, \quad n \neq k. \quad (4)$$

Here L is the length from the box boundary conditions which are used for continuum states, it will obviously vanish in calculation, since $M_{nkcont} \sim \frac{1}{\sqrt{L}}$.

The first order correction for the envelope wavefunction is

$$\eta_n^{(1)} = e\hbar B \left(j_n + \frac{1}{2} \right) \sum_{k \neq n} \frac{M_{nk}}{E_n^{(0)} - E_k^{(0)}} \eta_{k0}, \quad n \neq k. \quad (5)$$

Again we can separate the influence of bound and continuum states in the sum, hence (5) is referred to the bound state, while for continuum states we have:

$$\eta_{ncont}^{(1)} = e\hbar B \left(j_n + \frac{1}{2} \right) \frac{L}{\pi} \int_0^\infty \frac{M_{nkcont}}{E_n^{(0)} - E_k^{(0)}} \eta_{k0cont} dk_z, \quad n \neq k. \quad (6)$$

\hat{H}_{NP} is treated with second order perturbation theory in (2) and the corresponding energy correction amounts to:

$$\Delta E_{NP}^{(2)} = \left[(8j_n^2 + 8j_n + 5)\langle \alpha_0 \rangle + (j_n^2 + j_n + 1)\langle \beta_0 \rangle \right] \frac{e^2 B^2}{2\hbar^2}, \quad (7)$$

where $\langle \alpha_0 \rangle$ and $\langle \beta_0 \rangle$ are the expected values of nonparabolicity parameters (calculated with $\eta_{n0}(z)$ as basis functions).

The total energy and the envelope wavefunctions are given by

$$E = E_n^{(0)} + \Delta E_n^{(1)} + \Delta E_n^{(2)} + \Delta E_{ncont}^{(2)} + \Delta E_{NP}^{(2)}, \\ \eta_n = \eta_{n0} + \eta_n^{(1)} + \eta_{ncont}^{(1)}. \quad (8)$$

If an electric field is present along the QW growth direction then we have a linear in z term in the potential $V(z)$ in (1), which results in continuous energy spectrum. In the case of moderate external electric fields, the energy states that were previously bound evolve into the so-called quasi-bound states after the application of bias, and they can then still be treated as bound under the additional assumption that the potential is constant far enough from the well [10]. This consideration is exploited in our model to solve (1) in a simpler

manner than within a rigorous approach, which is rather cumbersome when nonparabolicity is involved. These quasi-bound states can be determined by numerical solving of the \hat{H}_0 eigenvalue problem and then the energy and the wavefunction corrections can be calculated. Separating the influence of bound states and continuum states is not possible in that case.

Equations (1) – (8) represent the complete model of the second order perturbation theory of NPE in semiconductor nanostructures, with a remark that (4) and (6) cannot be written (also (8) is slightly changed) if electric field is present.

As shown in [4] this model is applicable for energies under $5/9$ of the maximum energy value of:

$$E_{max} = \frac{\hbar^4}{16|\alpha_0|(m^*)^2}. \quad (9)$$

For GaAs with parameters from [2] E_{max} is 384 meV and we claim that this model is applicable up to E_{max} , not $5/9 E_{max}$. It also important to note that the application of perturbation theory also has constraints which can limit the value of applied external magnetic field. In this paper we will only focus on the constraint (9) and allow magnetic field to increase to 60 T. We will address the constraints of perturbation theory in further research.

3 Quantum Well Without Electrical Field

We now apply model the presented above on the finite QW. We consider a GaAs quantum well of width a surrounded by Al_{0.3}Ga_{0.7}As barriers of the height V_b with parameters from [2].

The potential $V(z)$ is symmetric, hence we can separate the energy spectrum into odd and even states. Solving eigenvalue problem of Hamiltonian \hat{H}_0 from (1) yields the unperturbed wavefunctions

$$\eta_{n0+} = \begin{cases} B_{n+} \cos(K_{n+} z), & |z| \leq a/2 \\ C_{n+} e^{-\lambda_{n+}|z|}, & |z| > a/2 \end{cases} \quad \eta_{n0-} = \begin{cases} B_{n-} \sin(K_{n+} z), & |z| \leq a/2 \\ C_{n-} e^{-\lambda_{n+} z}, & z > a/2 \\ -C_{n-} e^{\lambda_{n+} z}, & z < -a/2 \end{cases} \quad (10)$$

$$K_{n\pm} = \sqrt{\frac{m_1^*}{\alpha'_1 \hbar^2}} \sqrt{1 - \sqrt{1 - 4\alpha'_1 E_{n\pm}^{(0)}}}, \quad \lambda_{n\pm} = \sqrt{\frac{m_2^*}{\alpha'_2 \hbar^2}} \sqrt{\sqrt{1 + 4\alpha'_2 (V - E_{n\pm}^{(0)})} - 1}.$$

The index „+“ denotes even states, while the index „-“ denotes the odd ones; furthermore index 1 refers to the material of the well (GaAs) and index 2 to the material of the barrier (AlGaAs). Parameters $\alpha'_1, \alpha'_2 > 0$ represent the

modified nonparabolicity parameters as given in [2], while coefficients B_n and C_n are the normalization constants. The Hamiltonian \hat{H}_0 represents a 4th order differential equation, where only two solutions have physical meaning as shown in [4]. Eigenvalues of \hat{H}_0 are derived by using boundary conditions from [3]. By normalizing the wavefunctions $\eta_{n0\pm}$ from (10), and using boundary condition of continuity we can easily determine the normalization constants.

We can now apply the perturbation theory in order to determine the first and second order corrections. The first correction for energy is given by (2) and substituting (10) in (2) gives the parallel mass in the form presented in [2].

The second order correction for energy due to the bound states is given by (3). Matrix elements M_{nk} , calculated with wavefunctions from (10) amount to

$$M_{nk}^\pm = B_{n\pm} B_{k\pm} \left[\frac{\sin\left(\frac{K_{k\pm} - K_{n\pm}}{2}a\right)}{m_1^*(K_{k\pm} - K_{n\pm})} \left(1 - \frac{\hbar^2 K_{k\pm} K_{n\pm}}{2m_1^*} (2\alpha'_1 + \beta'_1) \right) \right. \\ \left. \pm \frac{\sin\left(\frac{K_{k\pm} + K_{n\pm}}{2}a\right)}{m_1^*(K_{k\pm} + K_{n\pm})} \left(1 + \frac{\hbar^2 K_{k\pm} K_{n\pm}}{2m_1^*} (2\alpha'_1 + \beta'_1) \right) \right] \\ + \frac{\cos\left(\frac{K_{k\pm} - K_{n\pm}}{2}a\right) \pm \cos\left(\frac{K_{k\pm} + K_{n\pm}}{2}a\right)}{m_2^*(\lambda_{n\pm} + \lambda_{k\pm})} \left[\left(1 - \frac{\hbar^2 \lambda_{n\pm} \lambda_{k\pm}}{2m_2^*} (2\alpha'_2 + \beta'_2) \right) \right], \quad (11)$$

where $\alpha' = -\left(\frac{2m_1}{\hbar^2}\right)^2 \alpha_0 > 0$ and $\beta' = -\left(\frac{2m_1}{\hbar^2}\right)^2 \beta_0 > 0$ represent the modified nonparabolicity parameters from [2] calculated in the well (index 1) and the barrier (index 2).

It is clear that in the limit $n \rightarrow k$ equation (14) becomes equal to m_\parallel^* from [2] as expected. It is also important to note that the n and k states must have the same parity, if they differ in parity $M_{nk} = 0$ which is obvious from (3) and (1) (the operator $\hat{M}(z)$ influences the parity of the integrand in (3)). The second order correction for energy due to the continuum states requires that we first model the continuum states and then insert the corresponding wavefunctions into calculations of the matrix elements M_{nkcont} . These wavefunctions can be obtained by using the Schrödinger equation without NPE since the NPE model is applicable only up to the value of energy from (9), and continuum energies

are certainly above that limit. Basically we use the Hamiltonian \hat{H}_0 from (1) in which the parameter $\alpha_0(z)=0$ and apply the parabolic boundary conditions. These wavefunctions can also be separated depending on their parity

$$\begin{aligned}\eta_{k0cont+} &= \frac{1}{\sqrt{L}} \begin{cases} D_+ \cos(k_w z), & |z| \leq a/2 \\ \sin(k_z |z| + \theta_+), & |z| > a/2 \end{cases} \\ \eta_{k0cont-} &= \frac{1}{\sqrt{L}} \begin{cases} D_- \sin(k_w z), & |z| \leq a/2 \\ -\sin(-k_z z + \theta_-), & z < -a/2 \\ \sin(k_z z + \theta_-), & z > a/2 \end{cases} \\ k_z &= \sqrt{\frac{2m_2^*}{\hbar^2} (E_{kcont} - V_b)}, \quad k_w = \sqrt{\frac{2m_1^*}{\hbar^2} E_{kcont}}, \\ D_+ &= \frac{\sin\left(\frac{k_z a}{2} + \theta_+\right)}{\cos\left(\frac{k_w a}{2}\right)}, \quad D_- = \frac{\sin\left(\frac{k_z a}{2} + \theta_-\right)}{\sin\left(\frac{k_w a}{2}\right)}, \\ \theta_+ &= \text{atan}\left(-\frac{k_z}{k_w} \cot\left(\frac{k_w a}{2}\right)\right) - \frac{k_z a}{2}; \quad \theta_- = \text{atan}\left(\frac{k_z}{k_w} \tan\left(\frac{k_w a}{2}\right)\right) - \frac{k_z a}{2}. \end{aligned} \quad (12)$$

The matrix elements M_{nkcont}^\pm are calculated in the same manner as M_{nk}^\pm and also they are different from zero only if states have the same parity. Although the analytic result for M_{nkcont}^\pm exists (similar to (11)) the integral in (4) has to be calculated numerically. Also note that the box boundary condition yields L in (12) and it will obviously vanish when (4) is evaluated.

The first order corrections for the envelope wavefunction of the bound states are calculated from (5) (after replacing (11)) and (6) (after replacing M_{nkcont} calculated with wavefunctions from (12)).

Energy correction due to the nonparabolic Hamiltonian is given by (7), and the expected values of the parameters α_0 and β_0 amount to

$$\langle \alpha_0^\pm \rangle = -\frac{\hbar^4}{4} \left[\frac{\alpha'_1}{m_1^{*2}} \left(\frac{a}{2} \pm \frac{\sin(K_{n\pm} a)}{2K_{n\pm}} \right) + \frac{\alpha'_2}{m_2^{*2}} \left(\frac{1 \pm \cos(K_{n\pm} a)}{2\lambda_{n\pm}} \right) \right] |B_{n\pm}|^2. \quad (13)$$

The same relation applies for $\langle \beta_0^\pm \rangle$ when β is inserted into (13) instead of α . Ekenberg has calculated these values approximately in [2], however (13) is the exact result.

Dipole matrix element is defined as

$$d_{if} = \int_{-\infty}^{\infty} \eta_i^* z \eta_f dz, \quad (14)$$

where index i refers to an initial state, and f to a final state of the optical transition. Envelope wavefunctions in (14) η_i, η_f are usually chosen as unperturbed wavefunctions. We will calculate the first order correction and use the form from (8). In this way we will be able to analyze the influence of magnetic field on the properties of our structure.

The quantum well under consideration has a width of 120 Å, with other parameters taken from [2], and accommodates 3 bound states at energies 25.1, 95.1 and 191.8 meV. By using (10) – (14) we can calculate the dipole matrix element for transition $3 \rightarrow 2$, and the results are presented in Fig. 1.

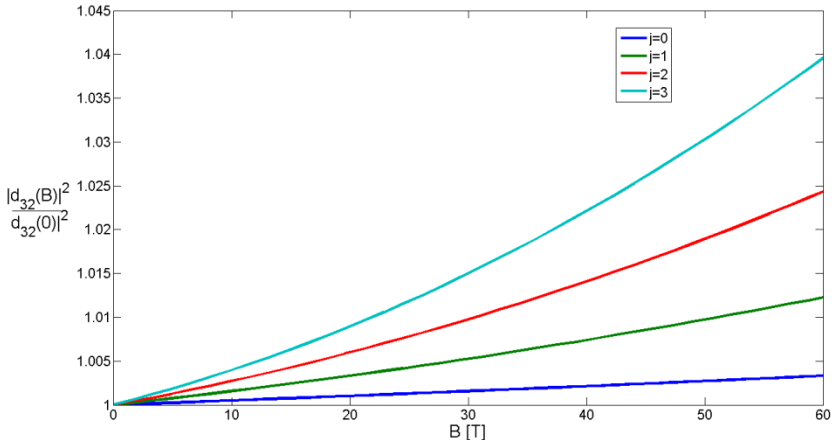


Fig. 1 – Dipole matrix depending on magnetic induction for different Landau levels (Landau level indices for both states are equal).
 $|d_{32}(0)| = 30.9 \text{ \AA}$ represents value for $B=0\text{T}$.

Fig. 1 illustrates the influence of magnetic field on $|d_{32}|^2$. Note that both levels can have arbitrary Landau index j_2 and j_3 , but we are interested only in transitions with the same indices, hence $j_2 = j_3 = j$. We can see that the magnetic field only slightly influences the value of the dipole matrix element (less than 1% up to 30 T) and this is the main reason why this effect is generally neglected in literature.

4 Quantum Cascade Laser

Applying our model to structures in the presence of electric field demands numerical solving of equations (1) – (9) (without (4) and (6)). We assume that a moderate electric field is applied and that we can approximate the potential at the structure ends with a constant [10]. The TMM method is used to determine the energies and wavefunctions of Hamiltonian \hat{H}_0 . These quasi-bound states are then used in the perturbation theory. Note that (9) gives a limiting energy with respect to the potential minima and in the structure of multiple QW this condition may constrain our model and question its applicability. Fortunately, as explained in [4], this model is applicable to multiple QW structures and equation (9) refers to the local potential minima in which the considered state is localized.

The gain of QCL depends on the squared modulus of dipole matrix element. We consider 3 states in QCL structure $E_1 < E_2 < E_3$, where two transitions are of interest: $E_3 \rightarrow E_2$ (lasing transition) and $E_2 \rightarrow E_1$ (transition for depopulation of the second state). Most models of QCL structures calculate (14) with unperturbed wavefunctions, thus the effect of external magnetic field cannot be seen. In this paper we will illustrate the dependence of the dipole matrix element on B for different Landau levels by using the wavefunctions with the first order correction in (14). This dependence arises from (5), but it must be calculated numerically.

For that reason we will apply our model to the mid- infrared (MIR) QCL proposed by Kruck in [11] who realized this structure experimentally and reported lasing at a wavelength of $\lambda \approx 11.3 \mu\text{m}$. Since this QCL has a GaAs/Al_{0.33}Ga_{0.67} active region, and nonparabolicity parameters from [2] are given for molar fraction of $x = 0.3$, we use linear interpolation to determine the corresponding values of these parameters. First we apply the TMM method to find the unperturbed energies and the wavefunction and the results of our simulations are presented in Fig. 2.

The numerically obtained lasing wavelength for this structure is $\lambda \approx 11.2 \mu\text{m}$, as shown in [4] and in Fig. 2. Under the influence of external magnetic field we calculate the corrections for energy and wavelength by using our model. The results are presented in Figs. 3 and 4, and depend on the value of the magnetic field and the Landau level index (for lasing optical transition, these levels are matched).

Fig. 3 shows how the lasing wavelength depends on magnetic field. This picture also shows how energy difference of these two levels change since the wavelength is $\sim 1/E_{32}$. We can see that the change is more rapid when higher Landau levels are considered.

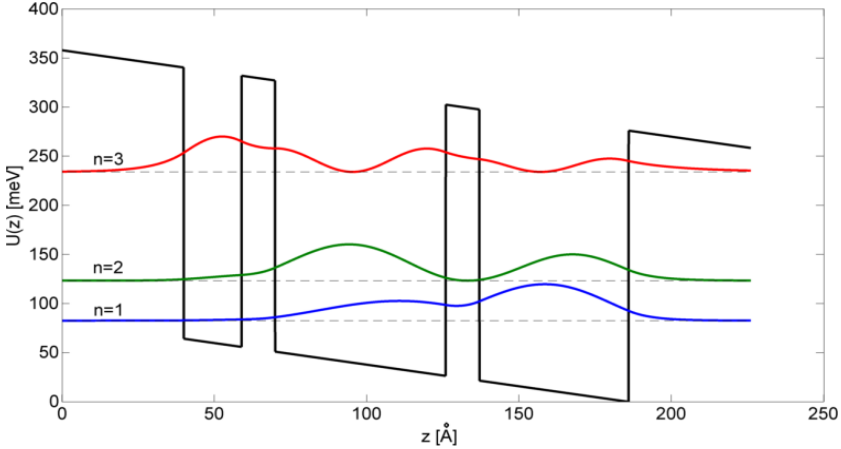


Fig. 2 – The active region of QCL [11] under an electric field of $K = 44$ kVcm $^{-1}$ and magnetic field of induction $B = 0$ T. The layer thickness starting from the left well are 19, 11, 56, 11, 49 Å. Relevant energies and the moduli squared of unperturbed wavefunctions are also displayed.

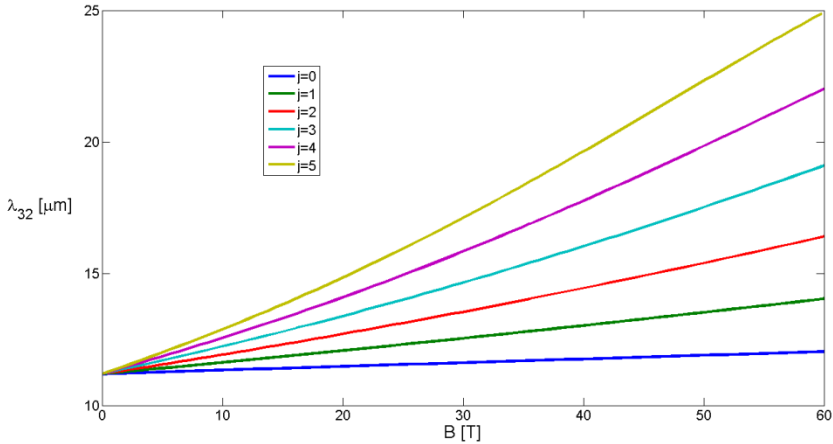


Fig. 3 – Lasing wavelength for structure from [11] depending on magnetic induction for different Landau levels.

Fig. 4 shows the dependence of the modulus squared of the dipole matrix element on magnetic field and also illustrates the effect since the dependence is compared to the case when there is no magnetic field (unperturbed value). It is interesting to note that for higher Landau levels we have rapid decreasing of $|d_{32}|^2$ which also represents the decreasing of the gain of the QCL structure. This effect is more pronounced than in the example from Fig. 1. We estimate that this effect may be even more pronounced in structures with higher NPE.

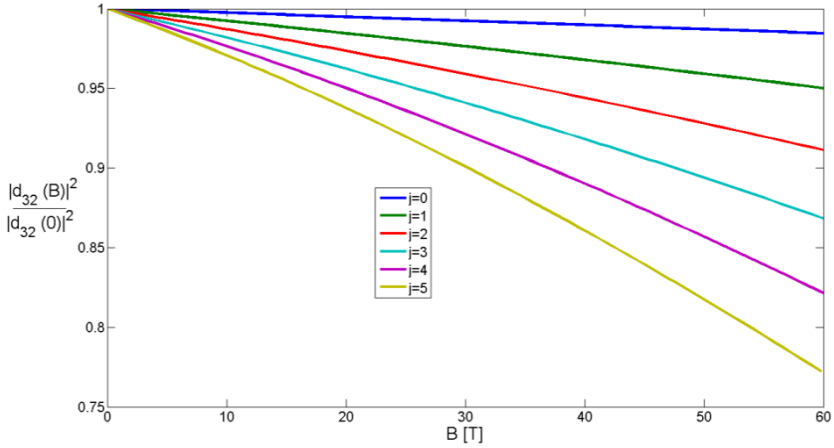


Fig. 4 – Dipole matrix element $|d_{32}|^2$ for structure from [11] depending on magnetic induction for different Landau levels, $|d_{32}(0)| = 26.02 \text{ \AA}$.

We can also calculate $|d_{21}|$ which describes the process of depopulation of the second laser state. Note that for $|d_{21}|$ Landau levels of both states can be arbitrary (as non-radiative scattering processes are considered) thus we will present cases $j_1 = j_2 = j$ (Fig. 5) and $j_1 \neq j_2$ (Fig. 6) separately.

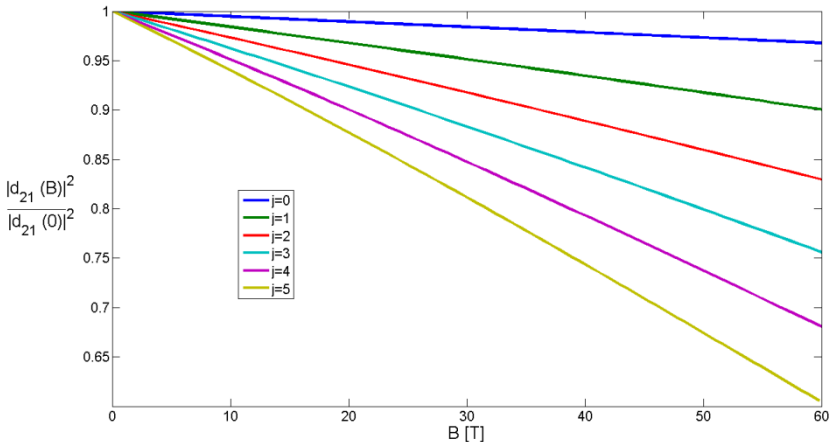


Fig. 5 – Dipole matrix element $|d_{21}|^2$ for structure from [11] depending on magnetic induction for different Landau levels (and $j_1 = j_2 = j$), $|d_{21}(B)| = 31.64 \text{ \AA}$.

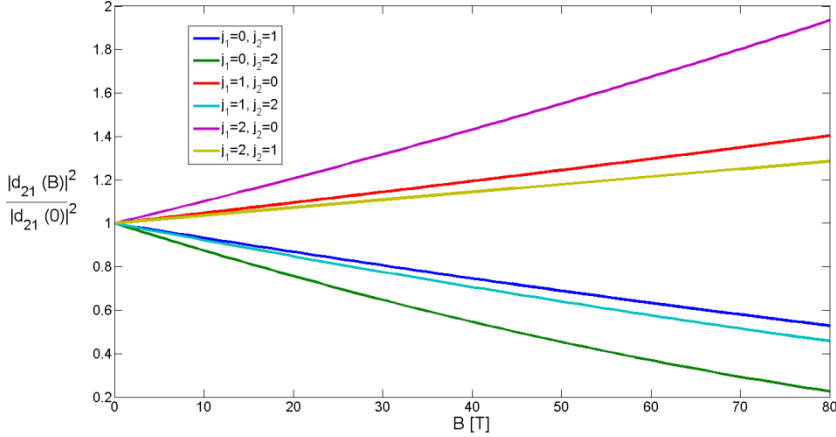


Fig. 6 – Dipole matrix element $|d_{21}|^2$ for structure from [11] depending on magnetic induction for different Landau levels (and $j_1 = j_2 = j_n$).

Fig. 5 shows how the modulus square of the dipole matrix element depends on magnetic field for the transition $2 \rightarrow 1$ when both states have same value of Landau level. The effect is also decreasing as in the transition $3 \rightarrow 2$ (Fig. 4), but is also more pronounced.

Fig. 6 depicts $|d_{21}|^2$ when Landau levels for particular states don't match. We can see that for $j_1 < j_2$ we have decreasing and effect is similar as in previous case, but for $j_1 > j_2$ this doesn't occur.

The gain of QCL is proportional to $|d_{32}|^2$ hence for low values of $|d_{32}|^2$ we might generally expect lower gain (if all other relevant factors are constant).

5 Conclusion

We have illustrated the effects of external magnetic field on the intersubband transition matrix element by using second order perturbation theory with the Hamiltonian which includes NPE. A suitable model (1) – (9) is formed which includes first^t order correction for envelope wavefunction and second order corrections for energy due to both bound and continuum states (in structures without the presence of external electric field). Application of the model to QW without the presence of external electric field yields analytic results (10) – (13) and the effects of magnetic field on dipole matrix element $|d_{32}|$ of an exemplary structure are presented.

When applied to a QCL structure, this model gives us new insights into effects of magnetic field on the matrix element which are usually neglected. We showed that the dipole matrix element can have a pronounced change for certain values of magnetic field and Landau level, which implies a change of gain of the structure in case of the lasing optical transition. It is interesting that for this transition for $j = 0$ the change is very mild, but the effect increases for higher Landau levels. In the case of the $2 \rightarrow 1$ transition, the combinations of Landau levels can be arbitrary as nonradiative transition takes place, with the incidence of the minimal value for $j_1 \leq j_2$.

6 Acknowledgement

This work was supported by the Ministry of Education, Science and Technological development (Republic of Serbia), (Project III45010) and NATO SfP Grant, ref. no. 984068.

7 References

- [1] M. Braun, U. Rossler: Magneto-optic Transitions and Non-parabolicity Parameters in the Conduction Band of Semiconductors, *J. Physics C: Solid State Physics*, Vol. 18, No. 17, June 1985, pp. 3365 – 3379.
- [2] U. Ekenberg: Nonparabolicity Effects in a Quantum Well: Sublevel Shift, Parallel Mass, and Landau Levels, *Physical Review B - Condensed Matter*, Vol. 40, No. 11, Nov. 1989, pp. 7714 – 7726.
- [3] V. Milanović, J. Radovanović, S. Ramović: Influence of Nonparabolicity on Boundary Conditions in Semiconductor Quantum Wells, *Physics Letters A*, Vol. 373, No. 34, Aug. 2009, pp. 3071 – 3074.
- [4] N. Vuković, J. Radovanović, V. Milanović: Enhanced Modeling of Band Nonparabolicity with Application to a Mid-IR Quantum Cascade Laser Structure, *Physica Scripta*, Vol. 2014, No. T162, Sept. 2014, p. 014014.
- [5] C. Gmachl, F. Capasso, D. Sivco, A.Y. Cho: Recent Progress in Quantum Cascade Lasers and Applications, *Reports on Progress in Physics*, Vol. 64, No. 11, Oct. 2001, pp. 1533 – 1601.
- [6] J. Faist, F. Capasso, D. Sivco, C. Sirtori, A. Hutchinson, A. Cho: Quantum Cascade Laser, *Science*, Vol. 264, No. 5158, April 1994, pp. 553 – 556.
- [7] A.A. Kosterev, F.K. Tittel: Chemical Sensors based on Quantum Cascade Lasers, *IEEE Journal on Quantum Electronics*, Vol. 38, No. 6, June 2002, pp. 582 – 591.
- [8] G. Wysocki, R. Lewicki, R. Curl, F. Tittel, L. Diehl, F. Capasso, M. Troccoli, G. Hofler, D. Bour, S. Corzine, R. Mualimi, M. Giovannini, J. Faist: Widely Tunable Mode-hop Free External Cavity Quantum Cascade Lasers for High Resolution Spectroscopy and Chemical Sensing, *Applied Physics B*, Vol. 92, No. 3, Sept. 2008, pp. 305 – 311.
- [9] J. McManus, J. Shorter, D. Nelson, M. Zahnister, D. Glenn, R. McGovern: Pulsed Quantum Cascade Laser Instrument with Compact Design for Rapid, High Sensitivity Measurements of Trace Gases in Air, *Applied Physics B*, Vol. 92, No. 3, Sept. 2008, pp. 387 – 392.

- [10] Z. Ikonić, V. Milanović: Semiconductor Quantum Microstructures, University of Belgrade, Belgrade, Serbia, 1997. (In Serbian).
- [11] P. Kruck, H. Page, C. Sirtori, S. Barbier, M. Stellmacher, J. Nagle: Improved Temperature Performance of $\text{Al}_{0.33}\text{Ga}_{0.67}\text{As}/\text{GaAs}$ Quantum-cascade Lasers with Emission Wavelength at $\lambda \approx 11 \mu\text{m}$, Applied Physics Letters, Vol. 76, No. 23, June 2000, pp. 3340 – 3342.